AIAA SPACE Forum
13 - 16 September 2016, Long Beach, California
AIAA/AAS Astrodynamics Specialist Conference

A New Method for Space Objects Probability of Collision

Austin B. Probe*
Texas A&M University, College Station, TX, 77843, USA
Tarek A. Elgohary†
University of Central Florida, Orlando, FL, 32816, USA
John L. Junkins‡
Texas A&M University, College Station, TX, 77843, USA

The state of a dynamical system and its uncertainty, as defined by its probability density function (PDF), are valuable for numerous fields in science and engineering. There have been numerous methods proposed to estimate and quantify this uncertainty. In astrodynamics, space situational awareness (SSA) is a major area that relies on uncertainty quantification to estimate a space object's state and its associated uncertainty. This data is invaluable for making informed decisions regarding probability of collision, tracking, and catalog maintenance. A new method for uncertainty quantification based on orthogonal polynomials and the application of Liouville's theorem is developed. The method identifies the region of extreme probability at the time of interest and populates that region with structured points. The associated PDF is computed based on the a-priori PDF of the initial conditions and/or the nominal values of the system parameters (e.g. drag coefficient). High dimension orthogonal polynomials are used to approximate the PDF at the target time. Having an analytical expression for the propagated PDF enables rigorous probabilistic analysis. The present method is applied to several problems to compute the probability of collision between two objects. Numerical experiments show orders of magnitude improvement in computational cost versus classical Monte Carlo Methods. The new approach is easy to implement, extensible to higher dimensions, computationally efficient and provides a rigorous approach to address probability of collision problems in SSA.

I. Introduction

The quantification of uncertainty (UQ) is a useful capability in fields ranging from signal processing to weather prediction to financial analytics. In astrodynamics, space situational awareness (SSA) relies extensively on UQ methods in order to accurately estimate resident space objects (RSOs) states. An accurate assessment of an RSO state uncertainty is vital to answering questions related to key SSA challenges, such as conjunction analysis, probability of collision or uncorrelated track association.[1–8] These challenges frequently require the use of probability methods which can be challenging when the probability density function (PDF) of interest is not Gaussian. Additionally, many problems that begin with a Gaussian PDF require the uncertainty after long periods of propagation. As a result, the PDF warps and becomes non-Gaussian.[9] This can be seen in figure 1, which shows evolution of a Monte Carlo analysis for an orbit with one million samples over ten days, with the initial and final distributions shown in green and blue, respectively.

Commonly, the State Transition Matrix (STM) is used as a method of characterizing the posterior uncertainty. One approach is to compute first moment (mean) and second moment (covariance matrix) of the PDF and then use a conventional approach (Foster's method) to approximate the probability of collision.[10–12] This involves propagation of the STM in addition to the system states to the final time and

*Ph.D. Candidate, Texas A&M Aerospace Engineering, AIAA Student Member
†Assistant Professor, University of Central Florida Mechanical and Aerospace Engineering, AIAA Member
‡Distinguished Professor, Texas A&M Aerospace Engineering, AIAA Honorary Fellow

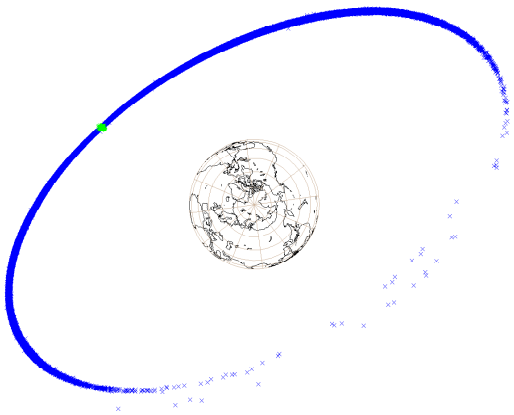

Figure 1. Monte Carlo Propagation Over Ten Days

linearly mapping the a-priori uncertainty to the final state space. This method has found wide adoption due to its simplicity and relatively inexpensive implementation cost. However, a significant flaw in the STM is that it relies on linearization of the system and assumes that the posterior PDF is Gaussian in nature. STM methods have been extended to account for higher order derivatives with State Transition Tensor methods.[13–15] These methods introduce the effects of higher derivatives to the mapping of the final PDF, however, they require either the computation or approximation of higher order partial derivatives.

As an alternative to the STM approach, the Fokker-Planck equation is known to capture the evolution of the initially Gaussian PDF in nonlinear dynamical systems.[16] Several works approached the UQ problem by solving the Fokker-Planck equation numerically in order to obtain the evolution of the PDF.[17–19]

The current standard method for high fidelity propagation of uncertainty is using Monte Carlo (MC) based methods. Using the a-priori distribution of the PDF, initial sample points are distributed throughout the state space. These points are then propagated forward in time to populate the distribution at the final time. The sample points from the final distribution can be used for generating statistical information regarding the final configuration, as was applied to conjunction analysis by Sabol et al. or to generate histograms or kernel density estimates to represent the posterior PDF.[20–22] MC based methods tend to be highly accurate, but suffer from the drawback of high computational cost. The accuracy has been shown to be inversely proportional to the square root of the number of sample points, as a result marginal increases in accuracy require the propagation of significantly more sample points.

Other recent UQ methods include Gaussian Mixture Models (GMMs) and Polynomial Chaos Expansions (PCEs). GMMs attempt to represent the PDF as a combination of Gaussian PDF components. GMMs can be used to build a representation of the initial uncertainty that can be propagated forward in time as individual Gaussian and then recombined to generate a posterior PDF.[21,23,24] However, this method assumes that the final PDF is well represented by the set of mixed Gaussians. The results of a Monte Carlo simulation can also be represented using GMMs to try and analyze the results.[25] Experiments have shown this approach to be superior to standard Monte Carlo with regard to computational cost to achieve a given tolerance as the dimension of the space increases. PCEs attempt to generate a functional representation of the system response that can be used for UQ in a fashion similar to results form MC.[26,27] PCE methods have been applied to UQ in astrodynmics by Jones et al.[28]

All of these methods have various advantages and disadvantages, but one key failing that they all share is that none can provide a general description of the posterior PDF, especially at higher levels of uncertainty,

without extreme cost. The efforts presented here seek to fill that gap and provide a good answer to what the PDF looks like at the time of interest.

In this work a new method for propagating uncertainty through a general nonlinear dynamical model is developed. The model is constructed such that all of the model uncertainty is assumed to be embodied in a random vector of parameters. Initial state errors and the uncertain parameters are assumed to belong to specified (known) probability distributions. In lieu of MC methods or other methods devised to characterize uncertainty, an alternative idea that is more computationally efficient and a more accurate way to capture the probability density distribution of the errors is introduced. This method identifies the region of extreme probability at the time of interest and populates that region with structured points and identifies the associated probability based on the a-priori PDF. By this method, these controllably dense points throughout the state space lead to an approximation for the non-linearly distorted non-Gaussian PDF at an arbitrary time t with a rigorous relationship to the a-priori probability density, and therefore doing any probabilistic analysis reduces to operations on simple interpolation functions. Using the concept of marginal probability it is possible to "integrate out" the effects of uncertain perturbations to the relevant dimensions in state space to reflect model uncertainty in the marginal PDF of the remaining state variables.

The method is very "clean" when applied to a conservative system, however it requires a minor extension to accommodate non-conservative effects such as drag. Introducing a parametric description of perturbations allows non-conservative effects to be included in the approach by simply augmenting the state space vector by the vector of uncertain parameters in the perturbing force model. These uncertain parameters are assumed constant, but unknown, and therefore satisfy trivial differential equations (their time derivative is zero), and in the augmented space, create an initial value problem with the state and parameters satisfying a joint probability density function.

Numerical studies show orders of magnitude reduction in the required number of particle trajectories compared to Monte Carlo. Remarkably, this approach makes the low probability density region of the PDF be much more accurately defined (than is routinely feasible via Monte Carlo, due to slow convergence and the associated high computational cost; i.e., the curse of high dimensionality). Table 1 gives the probability of an event in the n dimensional distribution lying within the volume of the $1, 2, \ldots, 6\sigma$ ellipsoids. As is evident the most familiar $1, 2$, and 3σ probabilities degrade rapidly as the dimension of the space increases. It is vital to note that the minimum dimension state space for quantifying uncertainty in orbit mechanics is 4 (planar problem), even without considering any parametric uncertainty in the force model. This table also shows, even for the simplest model of a Gaussian PDF assumption, that for a 7 dimensional space, we must expect in excess of 10000 Monte Carlo samples to get one sample to land outside the .999 probability density surface. We can see that in high dimension spaces, Monte Carlo becomes essentially useless to identify probability density surfaces associated with extreme events.

Invoking orthogonal approximation theory makes it possible to efficiently generate a multidimensional (at least a seven dimensional space is required for a perturbed orbit propagation) function approximation of the PDF that satisfactorily defines these low probability regions at any specified point in time and this will greatly facilitate integration over sub-domains to, for example, determine probability of collision during conjunction assessment.

In section II an overview of Liouville theorem and Monte Carlo methods is introduced with application on a simple Duffing oscillator. Section III introduces the orthogonal probability estimation concept and its application to approximate the PDF of the Duffing oscillator. The probability of collision, sections

Table 1. Curse of Dimensionality

	$\mathbf{1\sigma}$	$\mathbf{2\sigma}$	$\mathbf{3\sigma}$	$\mathbf{4\sigma}$	$\mathbf{5\sigma}$	$\mathbf{6\sigma}$
1	0.682689	0.954500	0.997300	0.999937	0.999999	0.999999998
2	0.393469	0.864665	0.988891	0.999665	0.999996	0.999999985
3	0.198748	0.738536	0.970709	0.998866	0.999985	0.999999925
4	0.090204	0.593994	0.938901	0.996981	0.999950	0.999999711
5	0.037434	0.450584	0.890936	0.993156	0.999861	0.999999050
6	0.014388	0.323324	0.826422	0.986246	0.999659	0.999997243
7	0.005171	0.220223	0.747344	0.974884	0.999241	0.999992751

VI through VIII, utilizing the PDF approximation is then computed for various problems starting with a simple linear system, two dimensional Duffing based problems and finally on a four-dimensional planar orbit problem. Finally, the results introduced are discussed and conclusions and future work are presented.

II. Monte Carlo Methods and Liouville's Theorem

In this section a review of both standard MC methods and Liouville's theorem is discussed. Relevant numerical examples are introduced for the Duffing oscillator problem that describes the baseline for the new UQ method.

II.A. Monte Carlo

MC methods, as mentioned above, quantifies a system uncertainty by generating initial samples based on the initial PDF. Each of theses samples is then propagated through the period of interest. The system response can then be quantified based on the density of the points within the state space. This quantification has historically been achieved using methods such as histograms and kernel density estimation.[21,22] The results of a one thousand simple MC analysis for the propagation of a Duffing oscillator for 3/4 of its undamped period (more details can be seen in section VI) are shown in figure 2. Figure 2(a) shows the distribution of the final system states from the MC propagation. Figure 2(b) shows the a histogram generated from the data and figure 2(c) shows the results of a kernel density estimate.

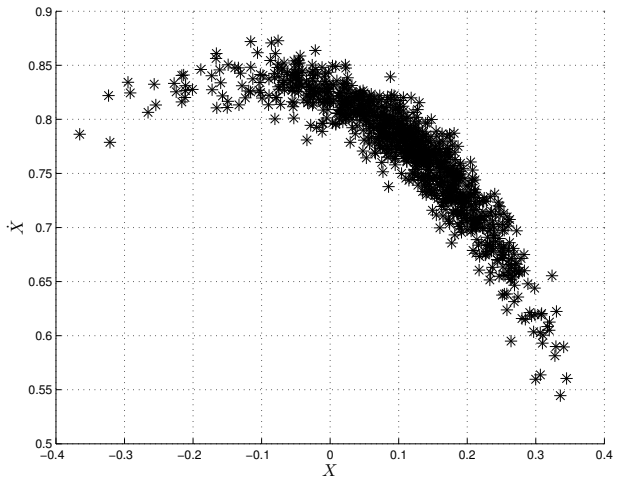

(a) MC Propigation Output

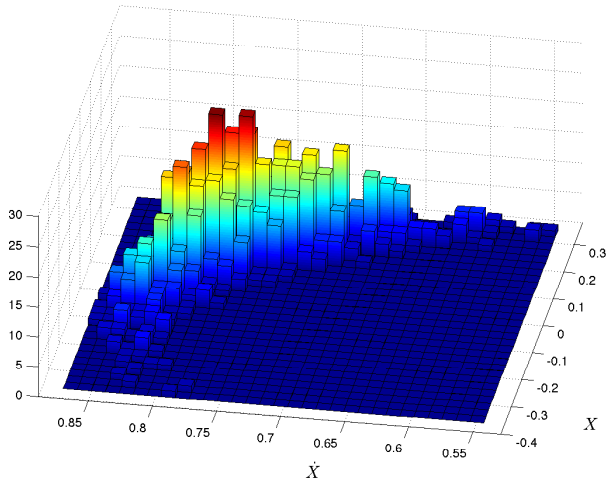

(b) Histogram Buit using MC

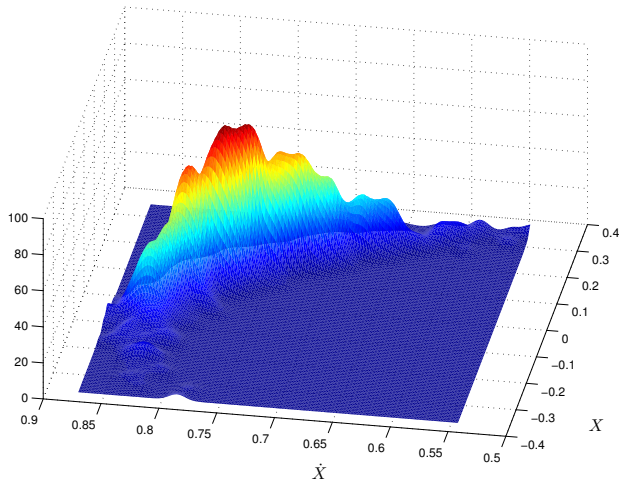

(c) Kernel Density Estimate using MC

Figure 2. Monte Carlo Analysis for a Duffing Oscillator

II.B. Liouville's Theorem

Liouville's theorem, named after the French mathematician Joseph Liouville, is a critical component of both statistical and Hamiltonian dynamics. The theorem is a consequence of Liouville's equation, Eq. (1), first recognized by J. W. Gibbs in 1884 based on identities derived by Liouville in 1838.[29,30] The theorem states that the density near a given system point moving through phase-space remains constant, independent of time.

$$\frac{d\rho}{dt} = \frac{\partial \rho}{\partial t} + \sum_{i=1}^{n} \left(\frac{\partial \rho}{\partial q_i} \dot{q}_i + \frac{\partial \rho}{\partial p_i} \dot{p}_i \right) = 0 \tag{1}$$

This theorem, when applied to probability density implies that the probability of a state, as defined by its initial conditions and a-priori PDF, remains constant as the state evolves along a trajectory through phase space. A flaw in standard MC methods is that they essentially disregard this probabilistic information associated with each trajectory. This disregarded information could otherwise contribute to improving the results from the analysis.

II.C. Liouville Monte Carlo

The a-priori probability information can be taken advantage of by treating probability space as a dimension to be explored during the MC analysis to create Liouville Monte Carlo (LMC). If a standard MC propagation algorithm has n states that are defined based on a normal distribution about the nominal, LMC will specify a probability value, p, based on a truncated normal distribution bounded by the probabilities of interest and then randomly select $n-1$ states and solve for the nth state based on the other states and p.[31] This process is trivial for an initial Gaussian probability, but requires slightly more effort for other PDFs. The value of p can then be used as a weighting factor for the determination of the final PDF. An example LMC propagation with the same setup as described in Section II.A is shown in figure 3. Initial qualitative analysis shows that the LMC results are smoother and better defined for the same number of points.

It is also possible to only consider a specified probability and use LMC to explore state space at that probability value, this feature is taken advantage of in Section VI and is considered the basis for the development of the present UQ approach.

III. Probability Analysis

Orthogonal probability approximation (OPA) promises to be at once a more computationally efficient and accurate way to capture the probability density distribution of the state uncertainty for an RSO. The new method deterministically places points at specified sampling locations at the final time and through back-propagation determines their probability based on a known initial probability density. The probability values at these points are then used to generate a multi-dimensional orthogonal approximation of the PDF.

IV. A Conceptual One Dimensional Example

OPA seeks to solve the quantification of uncertainty for a system at a time of interest, t_f, given a known distribution at some initial time t_0. This challenge is illustrated in figure 4 where the solid blue curve represents the known distribution at t_0 and the dotted green line represents the unknown distribution at t_f.

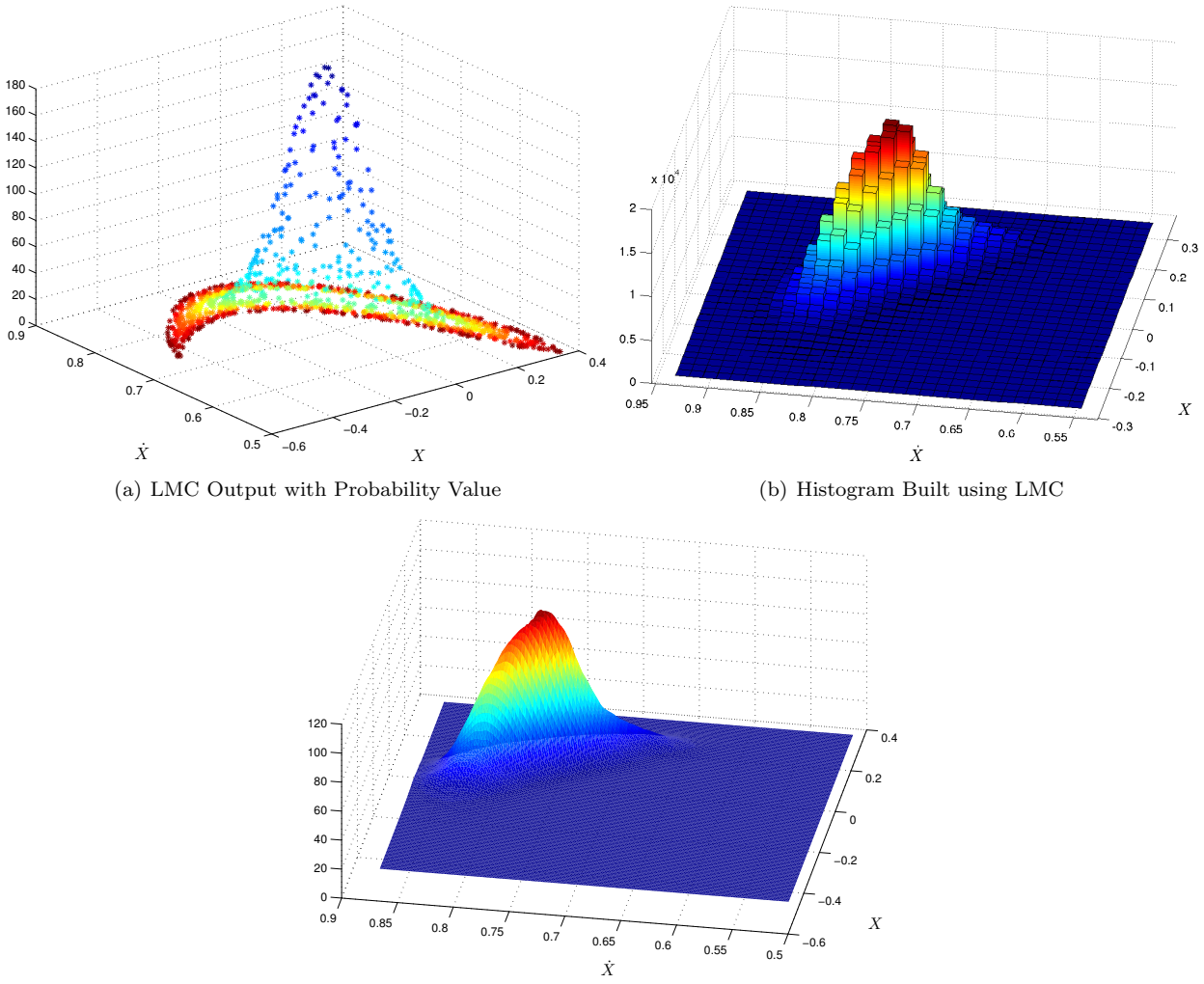

(a) LMC Output with Probability Value

(b) Histogram Built using LMC

(c) Kernel Density Estimate using LMC

Figure 3. Monte Carlo Analysis for a Duffing Oscillator

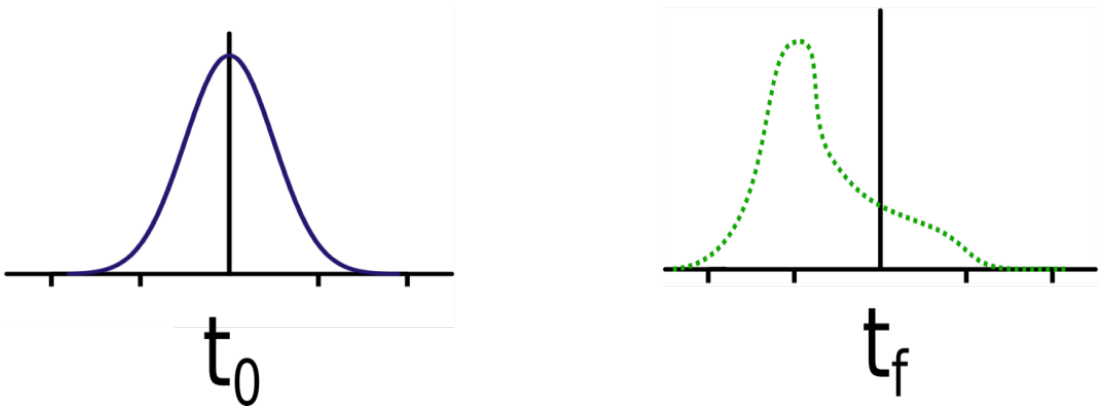

Figure 4. Uncertainty Quantification Problem

The initial step for OPA is to find the bounds of the region where the PDF must be approximated. This is achieved by computing the future values of a state trajectory whose immediate state exists at specified low value of the probability density. The future values along the state trajectory are calculated by propagating the ordinary differential equation (ODE) that defines the system up to t_f. This step is depicted in figure 5, where the small red lines show the different points along state trajectory at t_0 and t_f. The value of the probability density at this point is specified by the user, in this work a probability equivalent to 6σ in a Gaussian distribution. The region between these two points, or their generalized surface in higher dimensions, is said to be the region of extremal probability. Finding the initial points for the extremal probability is trivial for well characterized distributions (e.g. Gaussian or Cauchy) and if it is known that the initial distribution monotonically decreases on either side of its peak the points can simply be found using a gradient descent method. However, if the a-priori distribution does not meet these conditions a randomized search method would be required.

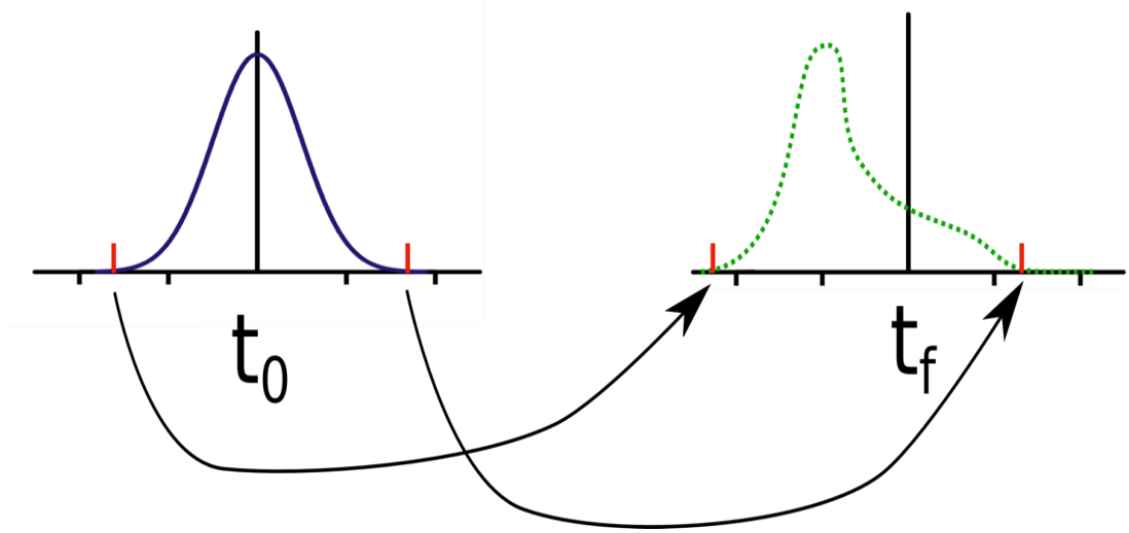

Figure 5. Propagation of the Extremal Probability Bounds

Once the bounds of the extremal probability region have been located at the time of interest, the space between them is populated with evaluation nodes. These nodes provide the samples for an approximation method. Figure 5 shows a distribution of cosine nodes placed between the extremal probabilities.

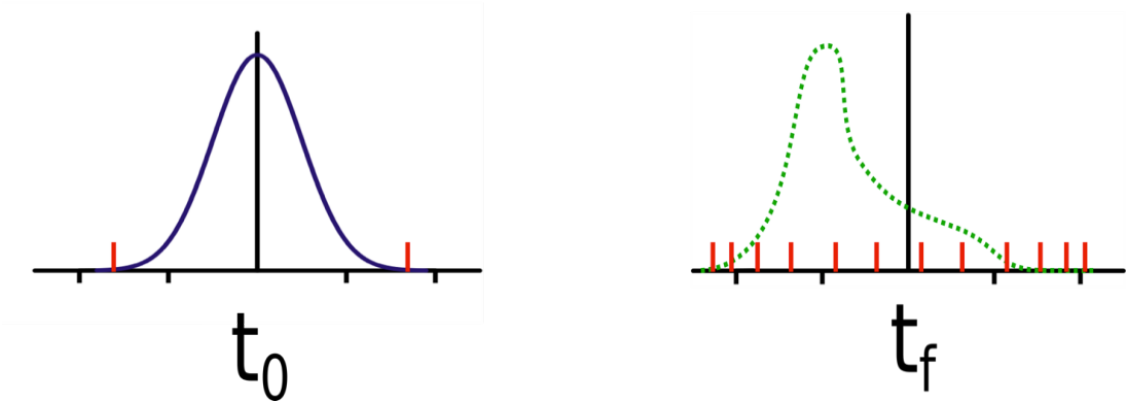

Figure 6. Evaluation Nodes Distributed at Posterior Time

For each of these evaluation nodes the corresponding state information is used as an initial condition

for back-propagation of the system to the initial time. The back-propagated state value is then compared to the a-priori probability distribution to get a value for the probability density at the final time. Once the evaluation nodes have been populated with values of probability density they are used to generate an approximation of the PDF at the posterior time. Figure 7 depicts the back-propagation from each of the evaluation nodes and figure 8 shows the resulting approximation for the posterior PDF.

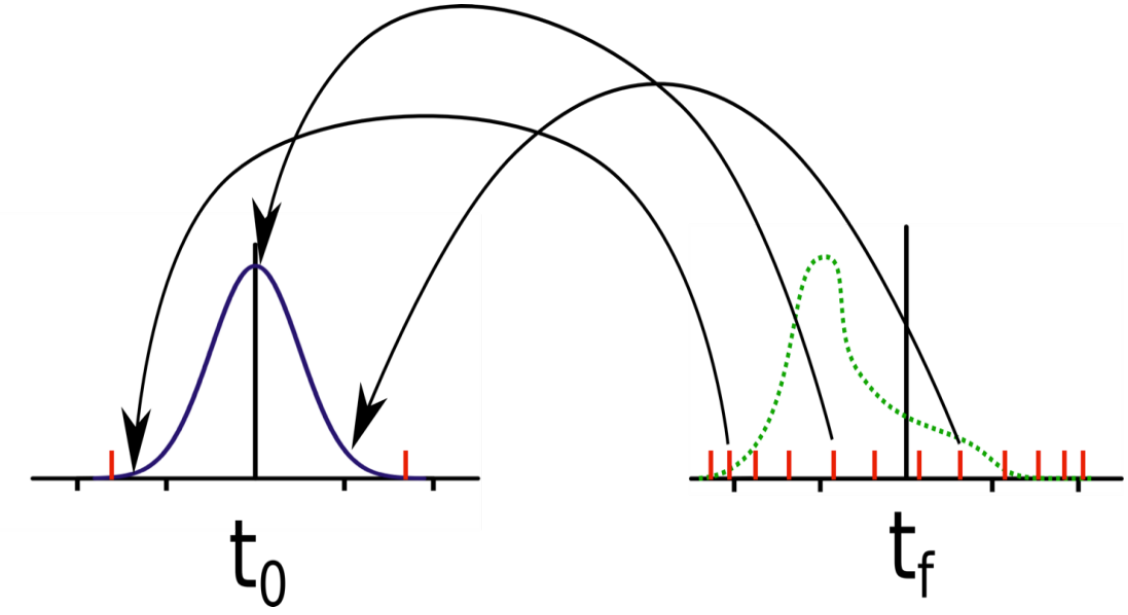

Figure 7. Back-propagation form the Evaluation Nodes to Determine the A-priori Probability Density

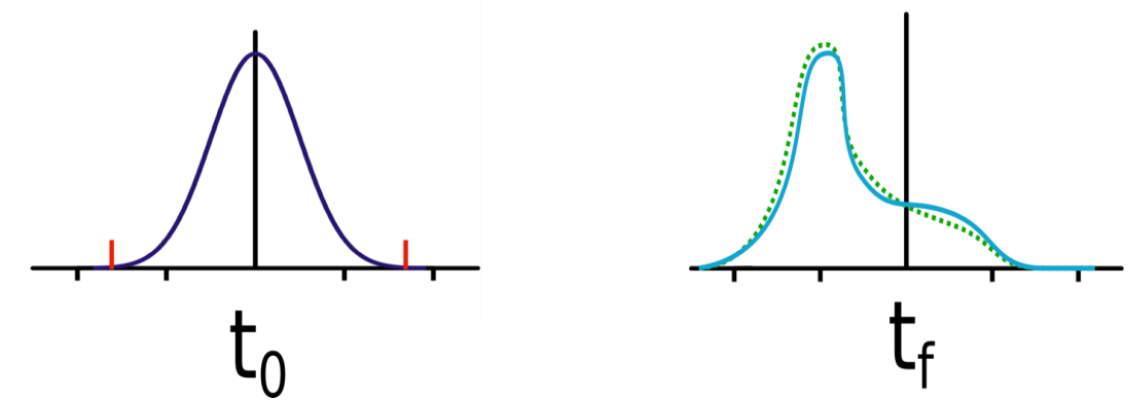

Figure 8. Probability Density Approximation Generated

IV.A. Orthogonal Probability Approximation for a Two Dimensional System

As depicted above, the new approach is straightforward for one dimensional systems. Invoking approximation theory allows the efficient generation of a multidimensional orthogonal function approximation of the PDF at any point in time.[32] To expand on the concept illustrated above, OPA is implemented for a simple two dimensional PDF for a single undamped duffing oscillator.

IV.B. Bounds of Extremal Probability

In order to determine the region of interest at t_f the extreme probabilities are propagated. For the two dimensional example it is tempting to sweep around the initial distribution, like sweeping through θ in a polar coordinate system, to identify the points with extreme probability. This would be analogous to selecting

the two points on either side of the distribution in the conceptual example, however, if the method is then extended into 3 dimensions one would be trying to evenly space points on a sphere. This challenge is known as Thomson problem, which originally dealt with finding the minimum energy configuration for electrons on a unit sphere.[33] This problem is famously unsolved, and that dose not even consider the difficulty when you move beyond 3 dimensions.[34] In light of this difficulty, a different method is devised that relies on a slightly modified version of LMC. Instead of spanning the entire probability space using LMC, points are only propagated along trajectories that originate from a surface where the value of the probability density matches the extreme value of interest. The results of this constant probability LMC can then be compared to find the bounds of the extremal region. This method requires the same order of forward propagation in two dimensions as the uniform method and is easily extensible to higher dimensions. Some small delta is added to maximum and minimum values used as the extremal probability region's bounds moving forward.

IV.C. Placement of Evaluation Nodes

The region of interest is then populated with the evaluation nodes. These nodes can be any grid of points associated with an approximation scheme, e.g. Gauss-Legendre, Chebyshev-Gauss-Legendre (CGL), Legendre-Gauss-Lobatto (LGL) nodes. This example relies on standard Chebyshev polynomial approximations, so a multidimensional cosine/CGL set of nodes is used. Figure IV.C shows extreme probability bounds in red and the resulting selected region of interest with an overlaid cosine grid.

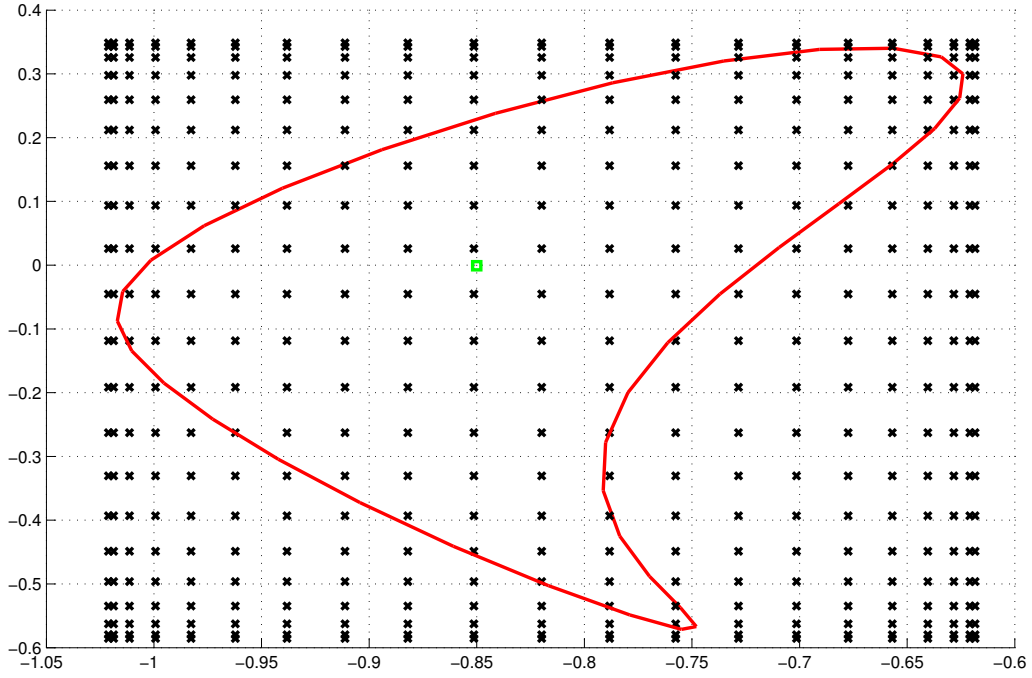

Figure 9. Region of Interest with Overlaid Cosine Grid

IV.D. Back-propagation and Approximation

At each of these evaluation nodes, the system is back-propagated from t_f to t_0 and the probability density is recorded as the probability density of the corresponding point at t_0 based on the a-priori PDF. These probability density values are then used to generate a 2D Chebyshev approximation for the PDF using simple orthogonal function approximation steps as,[32]

$$
\begin{aligned}
&p\left(x,\dot{x}\right), \quad x_{\min} \leq x \leq x_{\max}, \quad \dot{x}_{\min} \leq \dot{x} \leq \dot{x}_{\max} \\
&\zeta(x) = -1 + 2\left(\frac{x - x_{\min}}{x_{\max} - x_{\min}}\right) \quad \eta(\dot{x}) = -1 + 2\left(\frac{\dot{x} - \dot{x}_{\min}}{\dot{x}_{\max} - \dot{x}_{\min}}\right) \\
&P(\zeta,\eta) \equiv p\left(x(\zeta),\dot{x}(\eta)\right) = \sum_{i=0}^{N_x}\sum_{j=0}^{N_{\dot{x}}} a_{ij}\phi_{ij}\left(\zeta,\eta\right)
\end{aligned}
\tag{2}
$$

where, $-1 \leq \zeta, \eta \leq 1$, follows the cosine sampling nodal distribution, ϕ_{ij} represents the 2D Chebyshev basis functions and $N_x, N_{\dot{x}}$ represent the number of cosine nodes used for the fit for x and $\dot{x}$, respectively. As a result of having the analytical representation of the PDF represented in Chebyshev polynomials and their known coefficients, computing the marginal probability of one of the dimensions becomes easy to implement. At each node along the dimensions other than the dimension currently being marginalized the polynomial approximation is integrated and the definite integral is evaluated at the bounds of the extremal probability region.

$$
P_\zeta(\zeta) = \int_\eta P(\zeta,\eta)\,\mathrm{d}\eta = \int_{-1}^{1}\sum_{i=0}^{N_x}\sum_{j=0}^{N_{\dot{x}}} a_{ij}\phi_{ij}\left(\zeta,\eta\right)\,\mathrm{d}\eta \tag{3}
$$

Following Clenshaw and Curtis integration scheme for Chebyshev polynomials, computing the integral in Eq. (4) is straightforward,[35,36]

$$
\int T_n(x)\,\mathrm{d}x = \begin{cases} \frac{1}{2}\left[\frac{T_{n+1}(x)}{n+1} - \frac{T_{n-1}(x)}{n-1}\right] & n \neq 1 \\ \frac{1}{4}T_2(x) & n = 1 \end{cases} \tag{4}
$$

V. PDF Approximation Results

Figure 10 and figure 11 show both the approximate PDF and the integration where the blue lines represent the approximation in the $\dot{x}$ direction and the green lines represent their integrals. The red line represents a polynomial approximation of the marginal probability along x resulting from the integration of $\dot{x}$. Finally, the magenta line represents the integral of this marginal probability to produce the total probability. As a necessary condition for accuracy, the total probability value for this integration should be one, because it corresponds to a full PDF, and the result achieved agrees to nine significant figures. This is significant, because unlike many other PDF propagation methods that enforce the total value be equal to one, this method simply recovers the appropriate value. To improve the fit performance and to assist with visualization, the approximations are generated on a pseudo-logarithmic scale, shown in Eq. (5), where 0=0 and 1=1.

$$
LogLike(x) = \frac{log_{10}(x+1)}{log_{10}(2)} \tag{5}
$$

V.A. Linear Validation

To validate the performance of the OPA, it is used to propagate the PDF for a linear oscillator with an initial Gaussian distribution, Eq. (6) and (7). The properties of the oscillator are presented in table 2 and the results of the OPA in figure 12. These results are then compared to the results of propagating the uncertainty using analytic linear error theory, and the resulting error is shown figure 13. The error exhibited by OPA, maximum $\approx 10^{-9}$, is in line with the tolerance of integration of 10^{-10} and is well beyond what is required for most probabilistic applications. If greater precision is need it can be achieved by increasing the order of the approximation and decreasing the tolerance of the numerical integration.

$$
\dot{x} = Ax \tag{6}
$$

$$
A = \begin{bmatrix} 0 & 1 \\ -k & 0 \end{bmatrix} \tag{7}
$$

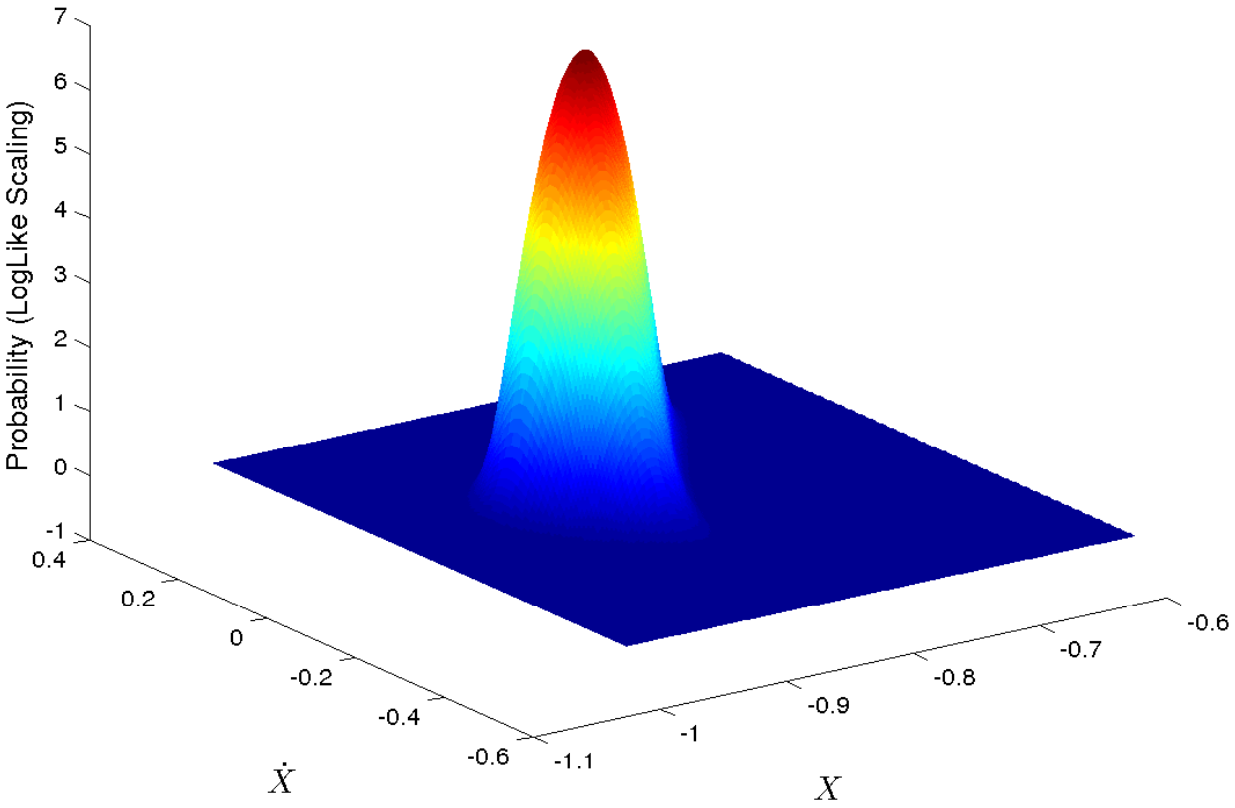

Figure 10. 2D PDF Approximation

Table 2. Linear Oscillator Properties

k	1
x_0	0.85
$\dot{x}_0$	0.0
t_f	3.2275 s
σ_x	0.03
$\sigma_{\dot{x}}$	0.05

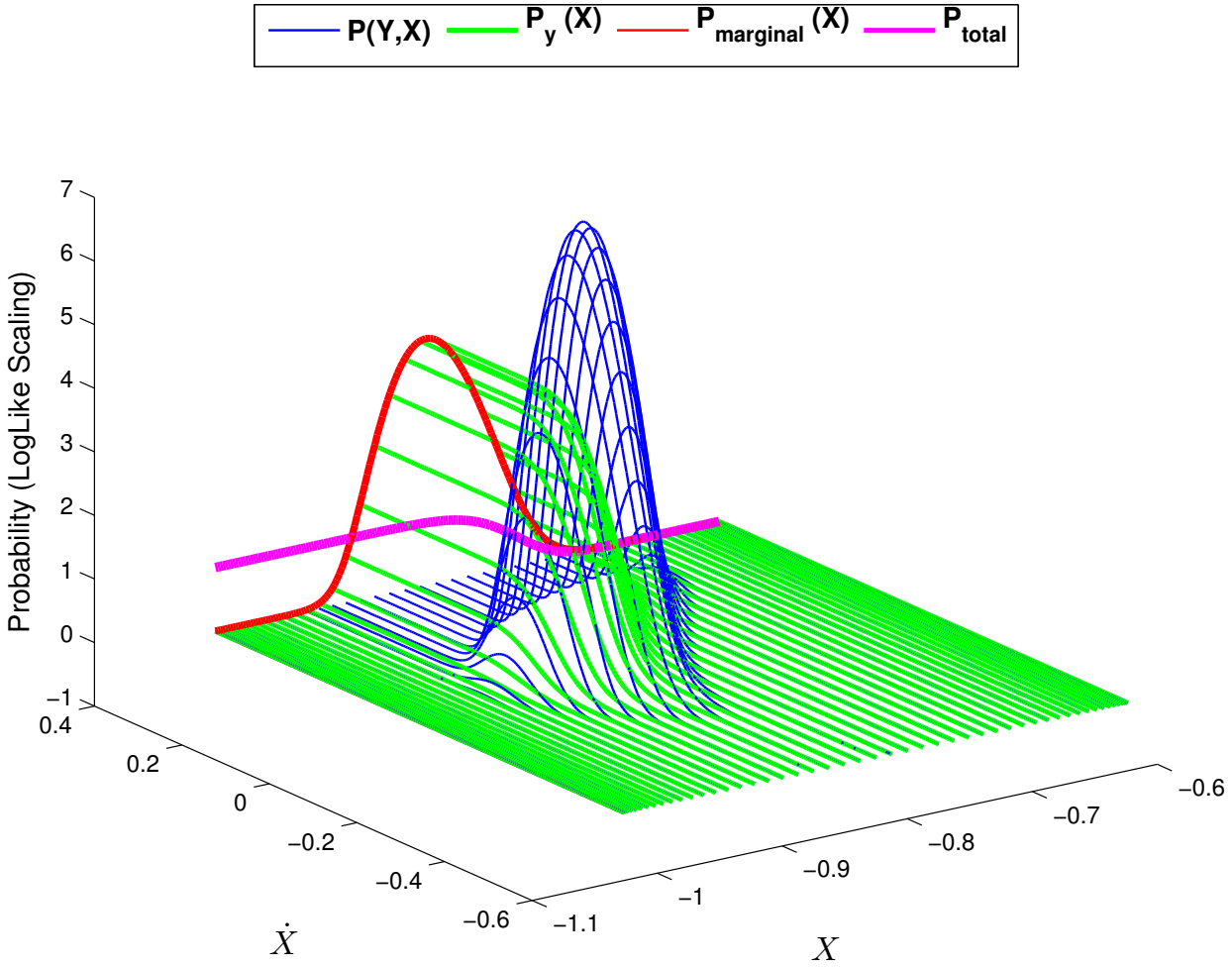

Figure 11. 2D PDF Approximation Integration

$$\dot{P} = AP + PA^T \tag{8}$$

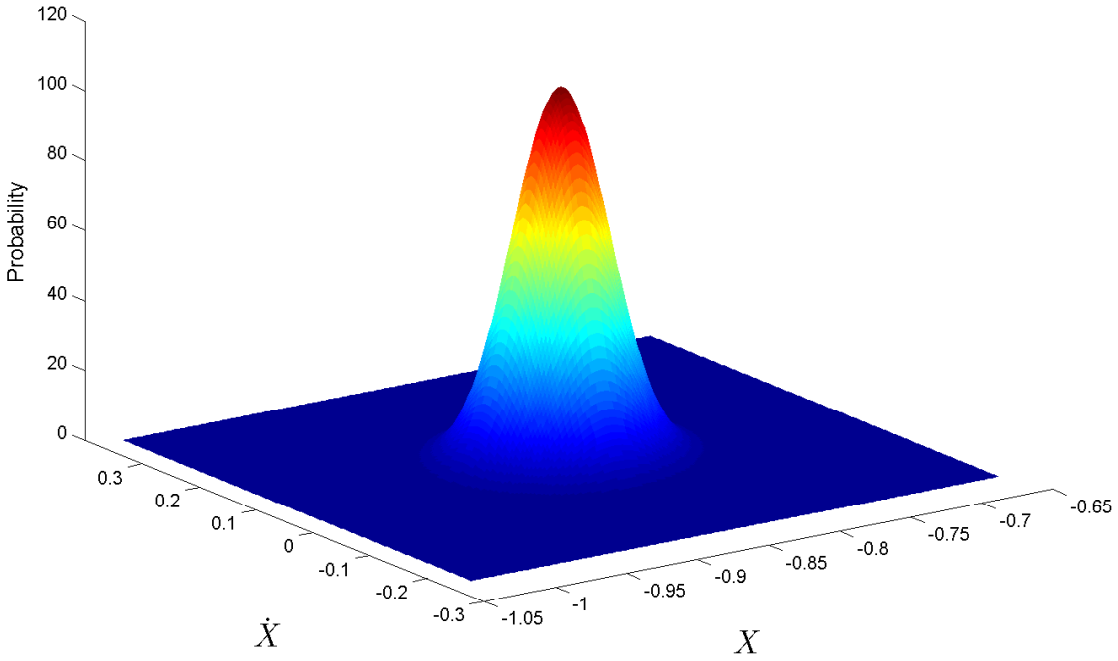

Figure 12. OPA PDF Approximation of Gaussian After Linear Propagation

VI. Collision Probability of Duffing Oscillators

To validate the present method for probability of collision analysis. it is useful to first examine a simplified problem using nonlinear Duffing oscillators. In view of the non-Gaussian nature of the PDFs this method abandons the Gaussian assumption completely and directly uses the computed non-Gaussian PDF approximation to compute probability of collision.

VI.A. Duffing Oscillators Properties

As a proof of concept the probability of collision for a pair of general Duffing oscillators with softening cubic nonlinearity given by,

$$\begin{aligned} &\ddot{x} + c\dot{x} + \omega^2 x - k^2 x^3 = 0, \qquad t_0 \leq t \leq t_f \\ &x(t_0) = x_0 \qquad \dot{x}(t_0) = \dot{x}_0 \end{aligned} \tag{9}$$

is explored. Randomly selected initial conditions and uncertainty following a isotropic Gaussian distribution with the properties laid out in in table 3 are used. For this conjunction analysis, uncertainty in the initial state (x and $\dot{x}$) is considered. This results in a 2D state space for the present UQ approach as presented in section III.

VI.B. Region of Possible Intersection

When an approximation for the full PDF was being considered in the previous section, the bound for the grid at the posterior time was selected based on the full range of probable values for the object. This requires

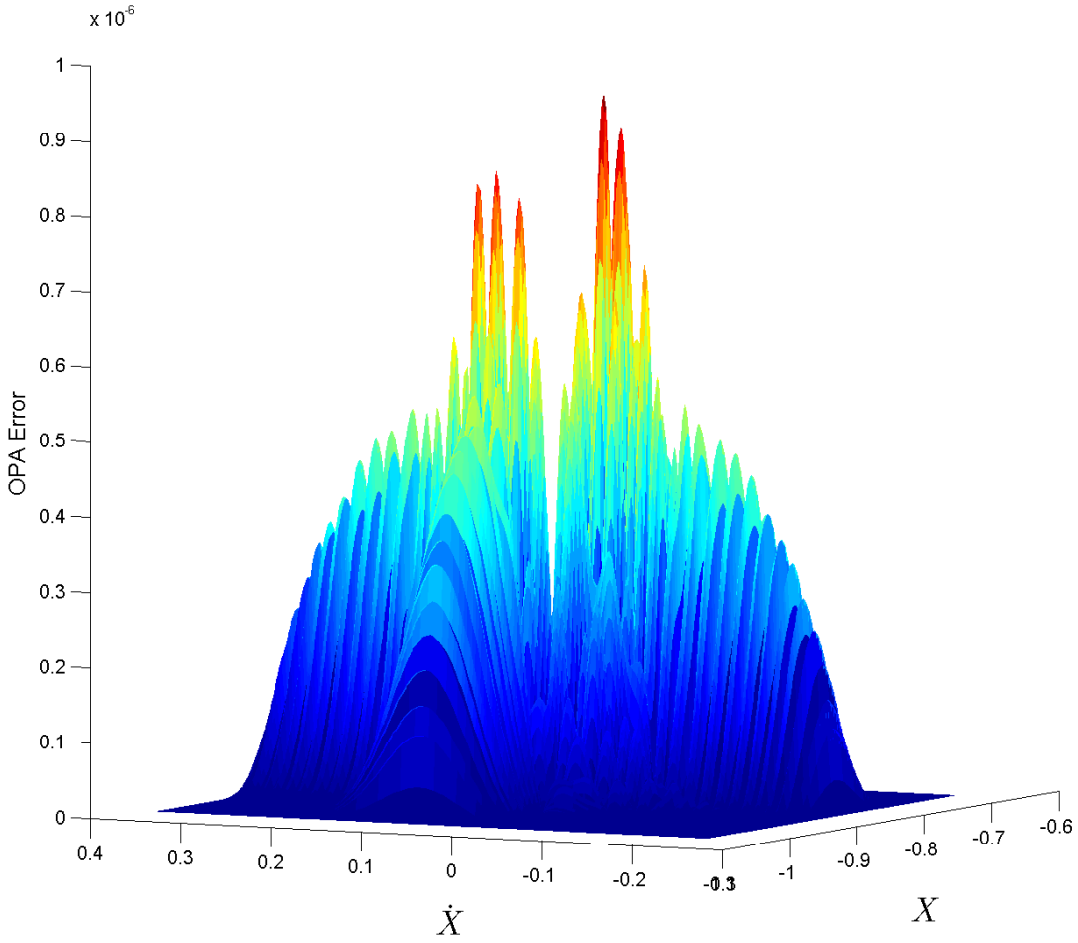

Figure 13. OPA vs. Analytic Propagation Error

the introduction of the concept of consequential and marginal dimensions. Consequential dimensions are those where the desired analysis is going to take place and marginal dimensions are the dimensions of the system state space that will be marginalized into the consequential dimensions. Now that the conjunction of two one dimensional oscillators is being examined the consequential dimension is the spatial dimension (x) whereas the velocity ($\dot{x}$) is the marginal dimension as its effect is marginalized into the spatial dimension. To find that region it is assumed that only areas in the consequential dimensions with a probability greater than some extreme probability should be examined, for this analysis the equivalent probability of Gaussian 6σ event is considered. The full region of the marginal dimensions must be considered because the entire region affects the consequential dimensions. The region where the grid is arranged is defined by the intersection of the 6σ equivalent contours for each of the objects of interest, as demonstrated in two dimensions in figure 14. Limiting the region of approximation to the space bounded by any possible collisions means that fewer grid points can be used to provide the same level of accuracy, reducing the cost of implementation. One attractive feature of OPA is that at this point if no region of intersection exists further analysis can be abandoned, avoiding the most computationally intensive components.

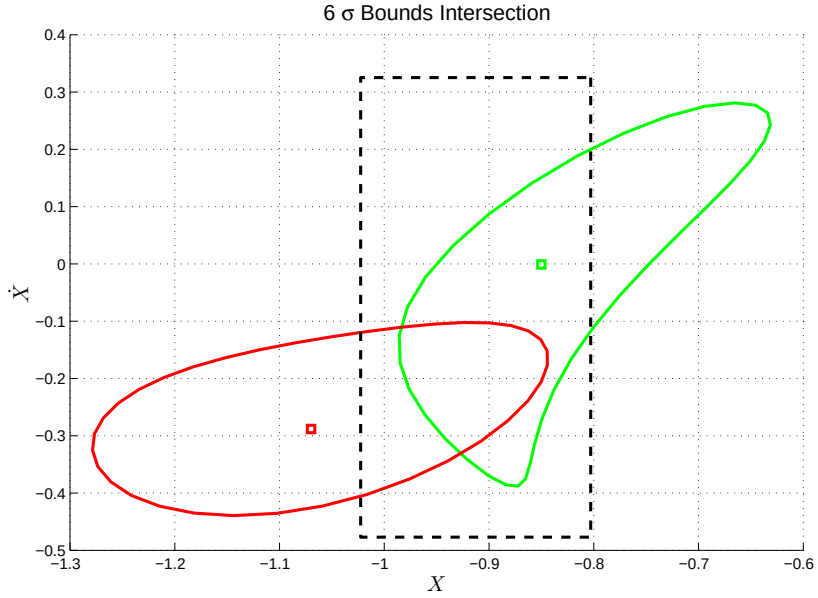

Figure 14. Intersecting Extremal Probability Region

VI.C. Probability of Collision

Similar to section III the region of possible intersection in both the consequential and marginal dimensions are populated with a 2D cosine grid. The probability values for each node are then evaluated via back

Table 3. Duffing Oscillator Properties

	Oscilator 1	Oscilator 2	Oscilator 3	Oscilator 4
c	0.0	0.0	0.0	0.0
k	0.7	0.7	0.7	0.7
ω	1.4	1.4	1.4	1.4
x_0	0.85	-1.85	-1.875	-2.0
$\dot{x}_0$	0.0	0.0	0.0	0.0
x_c	0.0	-1.3	-1.3	-1.5
σ_x	0.03	0.03	0.03	0.03
$\sigma_{\dot{x}}$	0.03	0.03	0.03	0.03

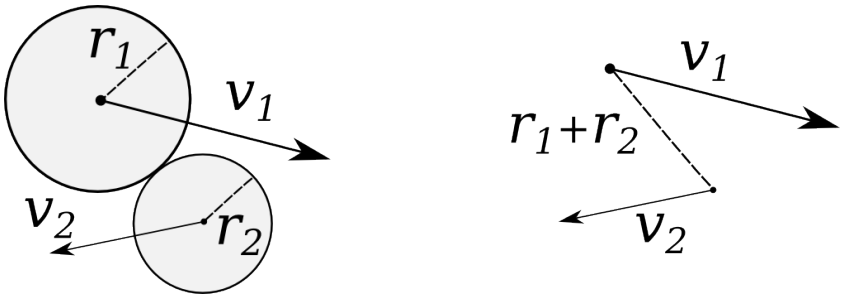

Figure 15. Radius of Collision

propagation and referencing the initial PDF. Using the same integration process, the probabilities for the velocities $\dot{x}_{1,2}$ can be marginalized into a pair of one dimensional PDFs for the positions x_1, x_2 for both objects, f_{x_1} and f_{x_2}. For the oscillators to collide they must come within a certain distance of one another, that distance is the sum of the radii of the mass at the end of the oscillators, or the so called radius of collision (r_{col}). The radius of collision concept is illustrated in figure 15. Traditionally, methods such as those discussed in section I construct a combined PDF from the uncertainty.

For any given point, the probability of collision

$$P(colision|x_1 = x) = \int_{x-\Delta x/2}^{x+\Delta x/2} f_{x_1}(\gamma)d\gamma \int_{x-r_{col}}^{x+r_{col}} f_{x_2}(\chi)d\chi \tag{10}$$

$$P(colision|x_1 = x) = f_{x_1}(x)\Delta x \int_{x-r_{col}}^{x+r_{col}} f_{x_2}(\chi)d\chi \tag{11}$$

$$g(x) = f_{x_1}(x) \int_{x-r_{col}}^{x+r_{col}} f_{x_2}(\chi)d\chi \tag{12}$$

$$P(colision|x_1 = x) = g(x)\Delta x \tag{13}$$

$$P(colision|(a \leq x \leq b)) = \int_a^b g(x)dx = \int_a^b f_{x_1}(x) \left(\int_{x-r_{col}}^{x+r_{col}} f_{x_2}(\chi)d\chi \right) dx \tag{14}$$

Then the joint probability for both oscillators occupying the same region defined by the radius r_{col} must be evaluated over the entire X region being considered. Using the X PDF approximations that have been generated for both oscillators and Clenshaw and Curtis integration (Eq. (4)) the joint probability of existence is evaluated for both oscillators at a set of cosine nodes over the integration bounds $\pm r_{col}$. A functional approximation for the probability of collision is constructed form the approximations of the PDF for X. This functional approximation is then integrated to provide the probability of collision.

An example of the probability of collision approximation, with total probability of collision is shown in figure 16.

VII. Validation

In order to validate the OPA method in providing accurate collision probability results, three cases for the Duffing collision problem are studied for various value of r_{col}. The three cases each have oscillator 1 interacting with oscillators 2-4, all propagated over 3/4 of the period of oscillator 1. For each case, MC simulations with one million randomly distributed sample points are propagated forward in time and the number of points lying within the collision region are counted to compute the MC based collision probability. OPA is computed following Eq. (10) through Eq. (14) in two sequences; Ob.1 representing the sequence in Eq. (14) and Ob. 2 representing the flipped sequence. The error results (using MC results as the truth) are shown in table 4 through table 9. As presented for all cases the agreement between the two methods is very good (up to 10 significant digits).

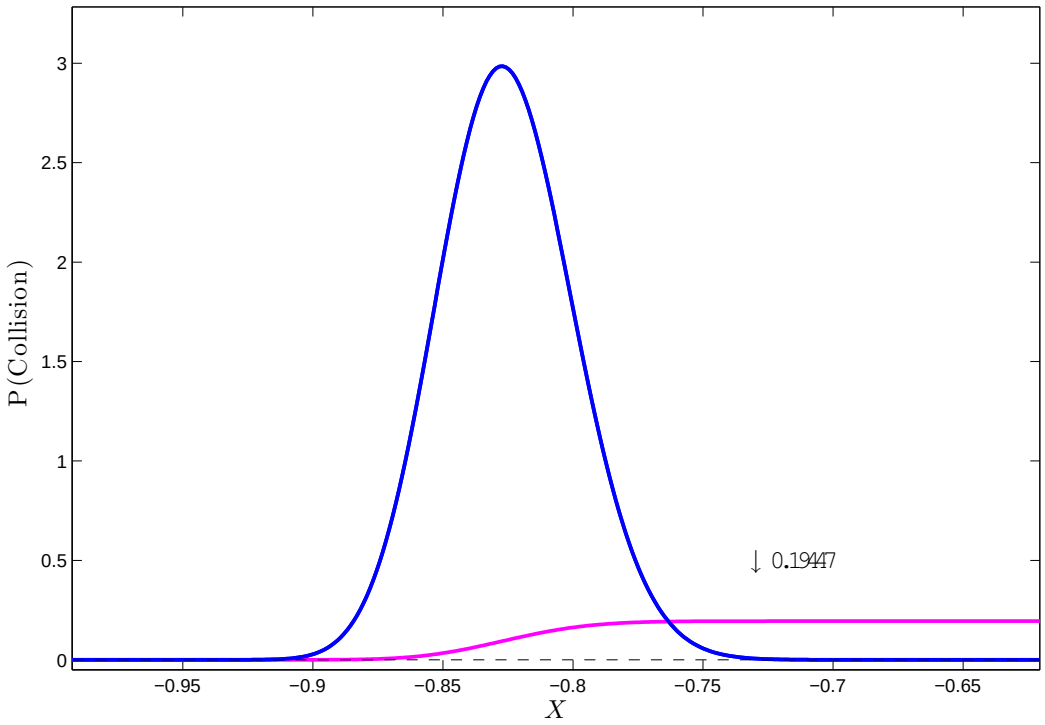

Figure 16. Probability of Collision

Table 4. Probability of Collision Results for $r_{col} = 0.01$

	MC	OPA Ob. 1	OPA Ob. 2
Case 1	1.24E-01	1.20E-01	1.20E-01
Case 2	6.17E-02	6.19E-02	6.19E-02
Case 3	1.53E-06	1.81E-06	1.81E-06

Table 5. Error of OPA vs. MC for $r_{col} = 0.01$

	% Err. Ob. 1	% Err. Ob. 2	% Agreement
Case 1	3.57E+00	3.57E+00	1.12E-10
Case 2	3.28E-01	3.28E-01	3.64E-11
Case 3	1.79E+01	1.79E+01	5.93E-04

Table 6. Probability of Collision Results for $r_{col} = 0.02$

	MC	OPA Ob. 1	OPA Ob. 2
Case 1	1.24E+00	1.20E-01	1.20E-01
Case 2	6.17E-02	6.19E-02	6.19E-02
Case 3	1.53E-06	1.81E-06	1.81E-06

Table 7. Error of OPA vs. MC for $r_{col} = 0.02$

	% Err. Ob. 1	% Err. Ob. 2	% Agreement
Case 1	4.31E+00	4.31E+00	1.89E-11
Case 2	3.09E-01	3.09E-01	1.98E-11
Case 3	9.63E+00	9.63E+00	5.67E-05

Table 8. Probability of Collision Results for $r_{col} = 0.03$

	MC	OPA Ob. 1	OPA Ob. 3
Case 1	1.24E+0-1	1.20E-01	1.20E-01
Case 2	6.17E-02	6.19E-02	6.19E-02
Case 3	1.53E-06	1.81E-06	1.81E-06

Table 9. Error of OPA vs. MC for $r_{col} = 0.03$

	% Err. Ob. 1	% Err. Ob. 2	% Agreement
Case 1	3.73E-01	3.53E-01	3.53E-01
Case 2	1.94E-01	1.94E-01	1.94E-01
Case 3	1.54E-05	1.59E-05	1.59E-05

VIII. Planar Orbit Collision

To evaluate the performance of orthogonal probability estimation to the UQ problems common to Space Domain Awareness the method was applied to the conjunction of a pair of satellites in the same orbital plane and in the absence of any perturbing forces. The orbits are depicted in figure 17 and their orbital elements, in Canonical units, are described in table 10. To construct a possible conjunction for analysis, a random point was chosen and the two objects were assigned velocities by slightly perturbing the required circular orbit velocity. The position of the second RSO was moved by a small distance perpendicular to its velocity vector to complete the close approach scenario. From these points the two RSOs were back-propagated, using Battin's analytical two-body method from the time of closest approach 100 TU to recover the nominal positions at the initial time.[37]

Table 10. Conjuncting RSO Parameters

	Orbit 1	Orbit 2
a	5.9278	4.4998
e	0.28180	0.33015
i	0	0
Ω	0	0
ω	0	0
M	5.0847	2.1840

At this point orthogonal probability estimation was applied to the four dimensional problem with an Gaussian a-priori uncertainty of 1e-6 DU in position and 1e-7 DU/TU in velocity. In order to find the region of intersection in higher dimensions, constant probability LMC (Section II) is used. Enough trajectories are propagated from uniformly distributed initial conditions with the defined extremal probability to define a region of the state space spanned by the reasonable terminal states of the objections being considered. Once this region of space has been defined for each oscillator the region of intersection can be defined. An example result of this process can be seen in figure VIII.

This constant probability LMC is carried out for to generate the probable region in the posterior state space in all four dimensions $(X, Y, \dot{X}, \dot{Y})$, the result of which is used to define the region in X and Y that will be populated with the approximation nodes, as shown in figure 19. The probability in the $\dot{X}$ and $\dot{Y}$ dimensions is then marginalized into the spatial dimensions for each RSO independently according to Eq. (3). The result is a pair of overlapping marginal probabilities defined at the specified approximation nodes as shown in figure 20.

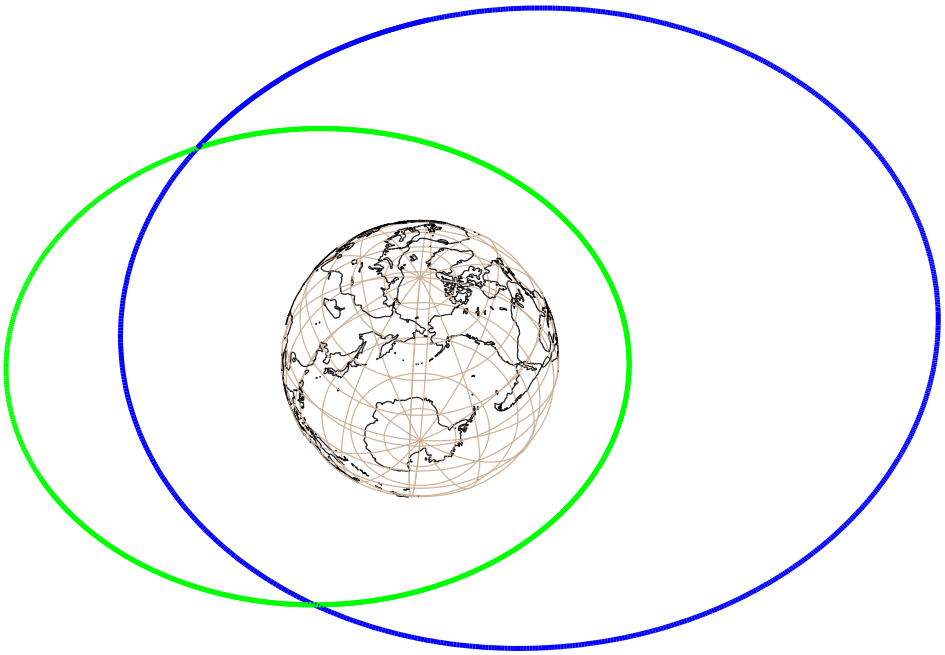

Figure 17. Planar Orbits Considered

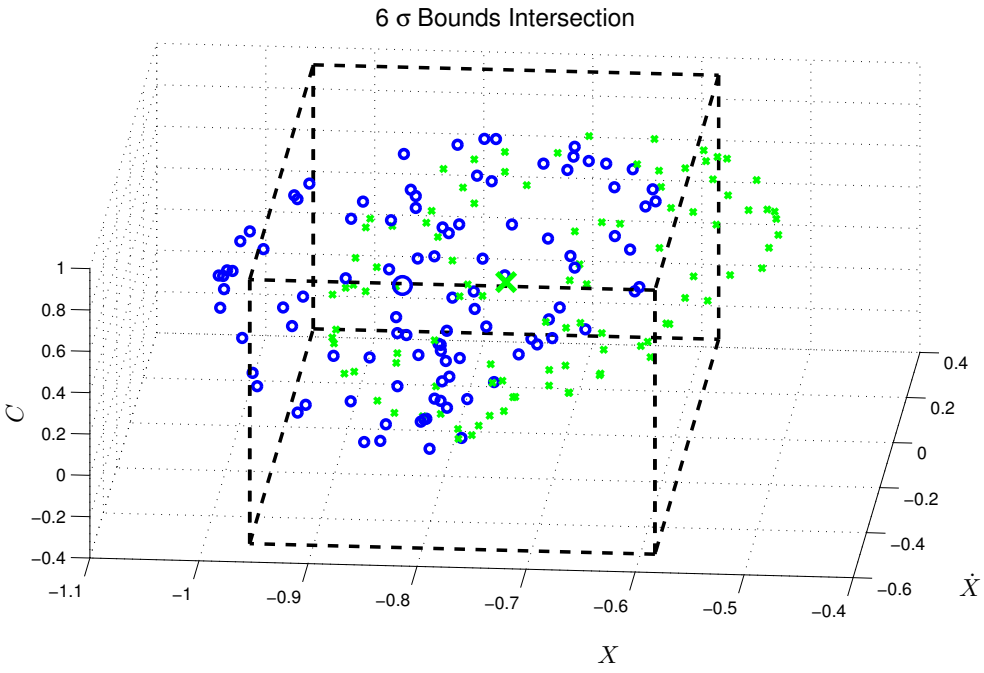

Figure 18. Intersecting Extremal Probability Region in 3D

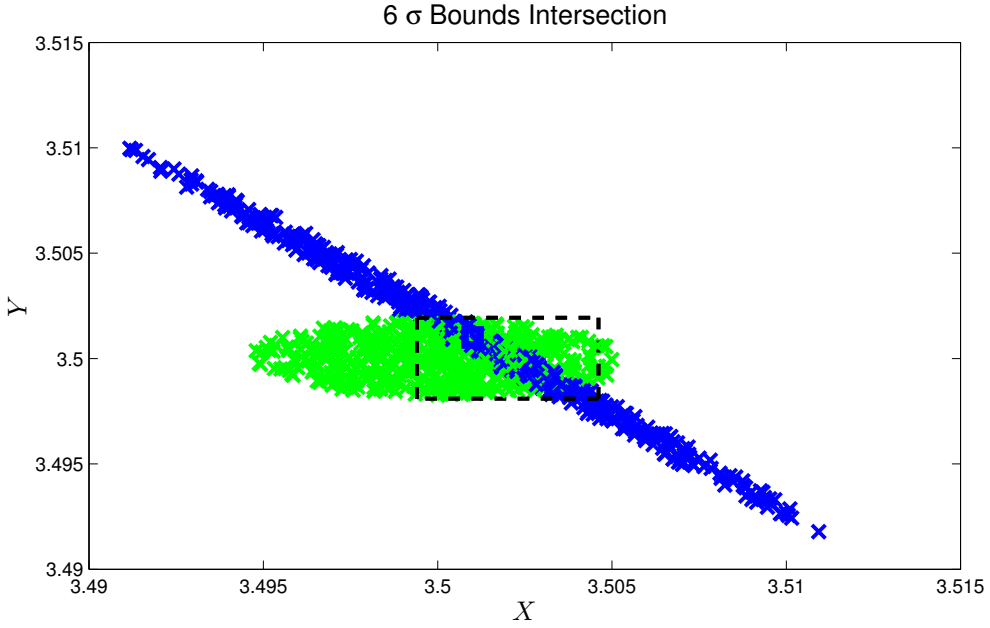

Figure 19. 6σ Orbit Intersection

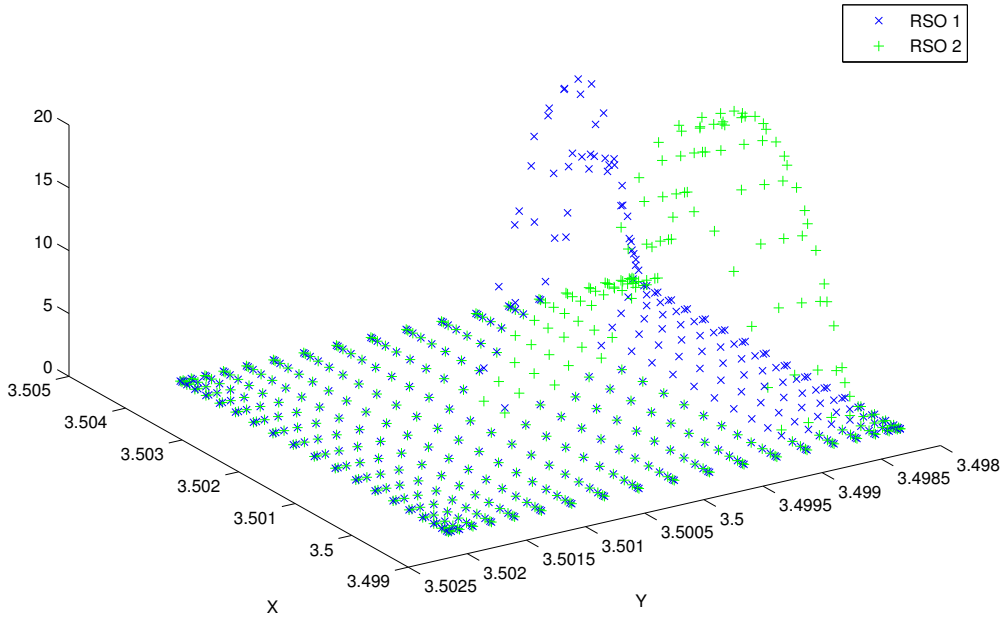

Figure 20. Overlapping RSO Marginal Probabilities

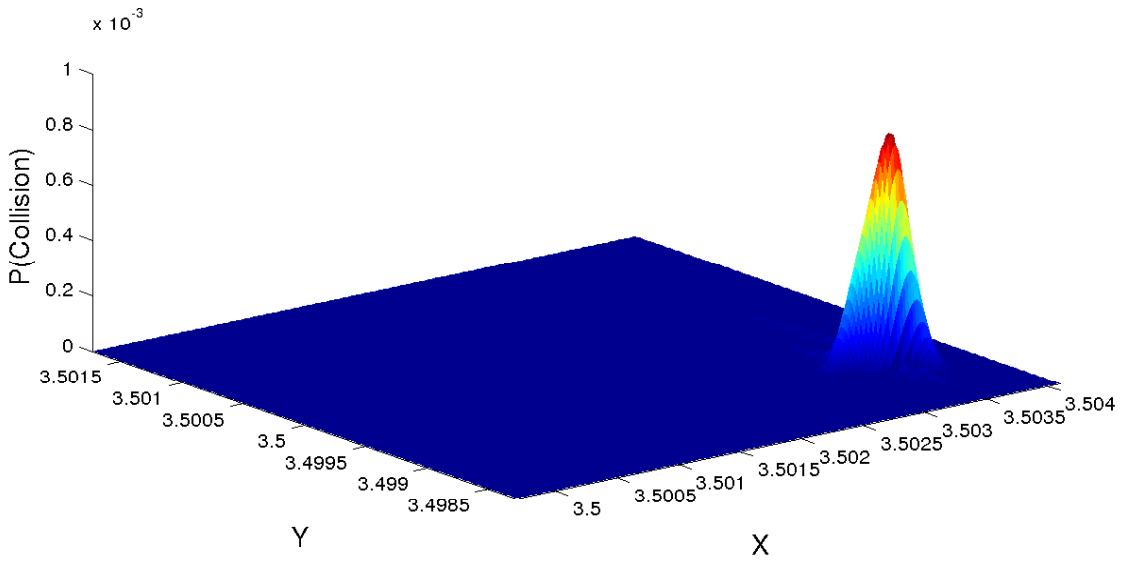

Figure 21. Probability of RSO Conjunction

These marginal probabilities in X and Y are used to generate approximations for the probability density of the RSOs over the region of interest. The local probability of collision, $P(colision|X = x, Y = y)$ is then computed as it was in section VI.C with the minor adjustment that the integral for f_{x_2} is then taken over circular areas defined by a r_{col} to generate an approximation for the probability of collision, as depicted in figure 21. Finally, the total probability of collision can be commuted by integrating over the resulting surface. These results are in the process of being validated with Monte Carlo methods similar to those presented section VII.

IX. Conclusions

A new method of uncertainty quantification, orthogonal probability estimation, was introduced that utilizes Liouville's theorem along with orthogonal polynomial approximations to generate representations of probability density functions. The approximate probability density functions can then be efficiently evaluated to answer questions related to the system's uncertainty. Additionally, some properties of the orthogonal approximations can be taken advantage of to easily and accurately preform commonly required tasks related to probability, such a marginalization.

This method was applied to provide several simple but representative problems from uncertainty quantification. A single probability density function for a duffing oscillator was approximated and used to demonstrate that the total probability of the posterior function was equal to one. The probability of collision for of a pair of damped Duffing Oscillators with uncertainty in the coefficient of damping was also considered. Finally, the method was used to compute the probability of collision for a pair of objects in planar orbits. This case demonstrates that orthogonal probability estimation can be effectively extended to address the challenges of uncertainty quantification in space domain awareness.

In future efforts, the validation of the planar case will be completed, the technique will be extended to the conjunction analysis in both a 5 dimensional planar case and a fully perturbed 7 dimensional case. Like many other methods for uncertainty quantification orthogonal probability estimation suffers form the curse of dimensionality, as such part of extending these efforts to higher dimensions will include the investigation of methods to mitigate this difficulty.

References

[1]Vallado, D., *Fundamentals of Astrodynamics and Applications*, Space Technology Library, 3rd ed., 2007.

[2]Alfano, S., "Review of conjunction probability methods for short-term encounters," *AAS paper*, , No. 07-148, 2007.

[3]Alfano, S., "Satellite conjunction monte carlo analysis," *AAS Spaceflight Mechanics Mtg, Pittsburgh, PA., Paper*, 2009, pp. 09–233.

[4]Carpenter, J. R., "Conservative Analytical Collision Probability for Design of Orbital Formations," *2nd International Symposium on Formation Flying*, 2004.

[5]Carpenter, J. R., "Non-Parametric Collision Probability for Low-Velocity Encounters," *Advances in Astronautical Sciences: AAS/AIAA Space Flight Mechanics Meeting*, 2007.

[6]Carpenter, J. R., Markley, F. L., and Gold, D., "Sequential Probability Ratio Test for Collision Avoidance Maneuver Decisions," *The Journal of the Astronautical Sciences*, Vol. 59, No. 1-2, 2012, pp. 267–280.

[7]Chesley, S. R. and Chodas, P. W., "Asteroid close approaches: analysis and potential impact detection," *Asteroids III*, 2002, pp. 55.

[8]Cho, D.-H., Chung, Y., and Bang, H., "Trajectory correction maneuver design using an improved B-plane targeting method," *Acta Astronautica*, Vol. 72, 2012, pp. 47–61.

[9]Junkins, J. L., Akella, M. R., and Alfrined, K. T., "Non-Gaussian error propagation in orbital mechanics," *Guidance and control 1996*, 1996, pp. 283–298.

[10]Foster, J. and Estes, H. S., "A parametric analysis of orbital debris collision probability and maneuver rate for space vehicles," *NASA JSC*, Vol. 25898, 1992.

[11]Akella, M. R. and Alfriend, K. T., "Probability of collision between space objects," *Journal of Guidance, Control, and Dynamics*, Vol. 23, No. 5, 2000, pp. 769–772.

[12]Chan, F. K., *Spacecraft collision probability*, Aerospace Press El Segundo, CA, 2008.

[13]Majji, M., Junkins, J. L., and Turner, J. D., "A high order method for estimation of dynamic systems," *The Journal of the Astronautical Sciences*, Vol. 56, No. 3, 2008, pp. 401–440.

[14]Turner, J. D., Majji, M., and Junkins, J. L., "High-order state and parameter transition tensor calculations," *No. AIAA-2008-6453, Honolulu, Hawaii, presented at AIAA/AAS Astrodynamics Specialist Conference*, 2008, pp. 18–21.

[15]Fujimoto, K., Scheeres, D., and Alfriend, K., "Analytical nonlinear propagation of uncertainty in the two-body problem," *Journal of Guidance, Control, and Dynamics*, Vol. 35, No. 2, 2012, pp. 497–509.

[16]Fuller, A., "Analysis of nonlinear stochastic systems by means of the Fokker–Planck equation," *International Journal of Control*, Vol. 9, No. 6, 1969, pp. 603–655.

[17]Kumar, M., Chakravorty, S., Singla, P., and Junkins, J. L., "The partition of unity finite element approach with hp-refinement for the stationary Fokker–Planck equation," *Journal of Sound and Vibration*, Vol. 327, No. 1, 2009, pp. 144–162.

[18]Sun, Y. and Kumar, M., "Numerical solution of high dimensional stationary Fokker–Planck equations via tensor decomposition and Chebyshev spectral differentiation," *Computers & Mathematics with Applications*, Vol. 67, No. 10, 2014, pp. 1960–1977.

[19]Vishwajeet, K., Singla, P., and Jah, M., "Nonlinear Uncertainty Propagation for Perturbed Two-Body Orbits," *Journal of Guidance, Control, and Dynamics*, Vol. 37, No. 5, 2014, pp. 1415–1425.

[20]Sabol, C., Binz, C., Segerman, A., Roe, K., and Schumacher Jr, P. W., "Probability of collision with special perturbations dynamics using the monte carlo method," *AAS/AIAA Astrodynamics Specialist Conference, Girdwood, AK*, 2011.

[21]Terejanu, G., Singla, P., Singh, T., and Scott, P. D., "Uncertainty propagation for nonlinear dynamic systems using Gaussian mixture models," *Journal of Guidance, Control, and Dynamics*, Vol. 31, No. 6, 2008, pp. 1623–1633.

[22]De Valpine, P., "Monte Carlo state-space likelihoods by weighted posterior kernel density estimation," *Journal of the American Statistical Association*, Vol. 99, No. 466, 2004, pp. 523–536.

[23]Horwood, J. T., Aragon, N. D., and Poore, A. B., "Gaussian sum filters for space surveillance: theory and simulations," *Journal of Guidance, Control, and Dynamics*, Vol. 34, No. 6, 2011, pp. 1839–1851.

[24]DeMars, K. J., Bishop, R. H., and Jah, M. K., "Entropy-based approach for uncertainty propagation of nonlinear dynamical systems," *Journal of Guidance, Control, and Dynamics*, Vol. 36, No. 4, 2013, pp. 1047–1057.

[25]Roscoe, C., Hussein, I., Wilkins, M., and Schumacher, P., "The Probabilistic Admissible Region with Additional Constraints," *Proceedings of the Advanced Maui Optical and Space Surveillance Technologies Conference, held in Wailea, Maui, Hawaii, September 15-18, 2014, Ed.: S. Ryan, The Maui Economic Development Board, id. 91*, Vol. 1, 2015, p. 91.

[26]Ghanem, R. and Spanos, P., "Polynomial chaos in stochastic finite elements," *Journal of Applied Mechanics*, Vol. 57, No. 1, 1990, pp. 197–202.

[27]Eldred, M. and Burkardt, J., "Comparison of non-intrusive polynomial chaos and stochastic collocation methods for uncertainty quantification," *AIAA paper*, Vol. 976, No. 2009, 2009, pp. 1–20.

[28]Jones, B. A., Doostan, A., and Born, G. H., "Nonlinear propagation of orbit uncertainty using non-intrusive polynomial chaos," *Journal of Guidance, Control, and Dynamics*, Vol. 36, No. 2, 2013, pp. 430–444.

[29]Gibbs, J. W., "On the Fundamental Formula of Statistical Mechanics, with Applications to Astronomy and Thermodynamicss," *Proceedings of the American Association for the Advancement of Science*, Vol. 33, 1884, pp. 57–58.

[30]Liouville, J., "Note sur la Théorie de la Variation des constantes arbitraires." *Journal de mathématiques pures et appliquées*, 1838, pp. 342–349.

[31]Robert, C. P., "Simulation of truncated normal variables," *Statistics and computing*, Vol. 5, No. 2, 1995, pp. 121–125.

[32]Junkins, J. L., Younes, A. B., Woollands, R. M., and Bai, X., "Picard Iteration, Chebyshev Polynomials and Chebyshev-Picard Methods: Application in Astrodynamics," *The Journal of the Astronautical Sciences*, Vol. 60, No. 3-4, 2013, pp. 623–653.

[33]Thomson, J. J., "On the structure of the atom: an investigation of the stability and periods of oscillation of a number of corpuscles arranged at equal intervals around the circumference of a circle; with application of the results to the theory of atomic structure," *The London, Edinburgh, and Dublin Philosophical Magazine and Journal of Science*, Vol. 7, No. 39, 1904, pp. 237–265.

[34]Smale, S., "Mathematical problems for the next century," *The Mathematical Intelligencer*, Vol. 20, No. 2, 1998, pp. 7–15.

[35]Clenshaw, C. W. and Curtis, A. R., "A method for numerical integration on an automatic computer," *Numerische Mathematik*, Vol. 2, No. 1, 1960, pp. 197–205.
[36]Mason, J. C. and Handscomb, D. C., *Chebyshev polynomials*, CRC Press, 2002.
[37]Battin, R., *An Introduction to the Mathematics and Methods of Astrodynamics*, AIAA Education Series, 2014.